

# Direct helium ion milling technology: towards the fabrication of extremely down-scaled graphene nanodevices

Shuojin Hang<sup>1</sup>, Zakaria Moktadir<sup>1</sup>, Nima Khalor<sup>1</sup>, Shinichi Saito<sup>1</sup> and Hiroshi Mizuta<sup>1,2</sup>

<sup>1</sup>Nano Research Group, University of Southampton, Southampton, Hampshire, UK. E-mail: sh13g08@ecs.soton.ac.uk

<sup>2</sup>School of Materials Science, JAIST, Nomi, Ishikawa, Japan. E-mail: mizuta@jaist.ac.jp

## 1. Introduction

Currently, the most established graphene device fabrication technique uses electron-beam (EB) lithography to pattern resist deposited on top of the graphene, followed by oxygen plasma etching [1,2]. However, parameters such as proximity effect, thickness uniformity of resist layer, and manual development of samples after e-beam lithography have limited the resolution of this method. Recently, a new patterning technique based on direct milling of graphene using a focused beam of helium ions generated in a helium ion microscope (HIM) has emerged [3,4]. In this work, we present our recent attempts of introducing an atomic-size helium ion beam to pattern graphene nanostructures directly (fig.1) and also investigate damage caused by helium ion bombardment onto carrier transport mechanisms in bi-layer graphene nanoribbons (GNRs).

## 2. Hybrid HIM/EB Fabrication Process

We exfoliated bilayer graphene flakes from highly oriented pyrolytic graphite onto heavily P-doped n-type Si substrate covered with 300nm SiO<sub>2</sub>. The number of layers was determined by Raman spectroscopy[5]. The coarse isolation patterns on graphene were first defined by EBL followed by 15 seconds etching in oxygen plasma. EBL-patterned source/drain electrodes were deposited by e-beam evaporation of 5nm Ti and 70 nm Au and a subsequent metal lift-off. Up to this point, graphene nanoribbons (GNR) down to 80nm wide can be prepared in this way with high reproducibility (fig. 2.a). The samples were annealed at 300 °C in forming gas (5% H<sub>2</sub> and 95% N<sub>2</sub>) for 1.5h for the removal of resist residues. In the last step, we milled the fine structure by scanning a highly focused helium ion beam within a small area on the GNR (fig.2. b). The accelerating voltage is tuned to be equal to the ‘best imaging voltage’ (~30kV) where the tungsten source emits the ions most effectively. Standard beam adjustment (e.g. beam tilt, beam align, wobble and stigmation) were performed to optimize the resolution. A dose test can be carried out on the nearby graphene flake. Usually a dose ranging from 0.6 to 1.5 nC/μm<sup>2</sup> is used, depending on the layer thickness, cleanliness and beam condition. Since the pattern generator in the HIM only exposes the

pre-defined ‘unmasked’ area, therefore the damage induced by the ion bombardment should be minimized.

## 3. Impact of He<sup>+</sup> induced point defects on carrier transport in bilayer GNRs

We systematically investigated the impact of beam-induced defects to graphene by measuring the conductivity of a bilayer graphene field effect transistor (BGFET) subject to precisely controlled He<sup>+</sup> irradiation (fig.3). From the D-peak analysis for Raman spectroscopy, it was shown that point defects (PDs) are induced by the He<sup>+</sup> irradiation [6]. Fig. 4(a) shows the resistance  $R = V_d/I_d$  ( $V_d = 7$  mV) of three BGTEFs as a function of the gate voltage and for three different channel widths: 20 nm, 50 nm and 200 nm and a similar length of 2 μm. Also shown is the resistivity of the BGFETs as a function of the channel width (Fig. 4(b)). This dependence is explained by a theoretical model which takes into account the diffusive scattering at the GNR channel edge, the short-range force scattering caused by PDs in the channel and the screened Coulomb scattering due to impurities at the GNR/SiO<sub>2</sub> interface. Helium ion bombardment was carried out in a 200 nm wide BGFET channel. In Fig. 5 we show the conductivity of the bombarded BGFET as a function of the gate voltage for different ion doses. The above mentioned theoretical model shows very good agreement with the experimental conductivity by reproducing the transition from sublinear (before irradiation) to linear (after irradiation of 4.16x10<sup>13</sup> ions/cm<sup>2</sup>) dependence of the conductivity on carrier concentration. From this analysis it is manifested that the dominant carrier transport mechanism changes from the diffusive edge scattering to PD scattering with an increase in He<sup>+</sup> dose. We evaluated that the concentration of induced PDs increases up to 5.2 x 10<sup>10</sup> cm<sup>-2</sup>. In addition we found for the BGFETs with the 200-nm-wide channel that the associated carrier mean free path (MFP) varies from 185 nm for the GNRs before irradiation, to 23 nm for those with He<sup>+</sup> dose of 4.16x10<sup>13</sup> ions/cm<sup>2</sup>, which corresponds approximately to the average distance between adjacent PDs.

## 4. Conclusion

We demonstrated an integrated fabrication process

of graphene nanostructures combining e-beam lithography and helium ion milling whereby  $<10\text{nm}$  resolution can be achieved. We also examined the impact of  $\text{He}^+$  irradiation on graphene. It was found that the resistivity of the channel increases with decreasing channel width as a result of the diffusive edge scattering. Introduction of point defects using the helium ion beam changes the dominant scattering mechanism from the diffusive edge scattering to the short-range scattering due to  $\text{He}^+$  induced PDs.

### Acknowledgment

The authors thank Dr S. Boden and Prof. D. Bagnall for their support to helium ion beam technology and Dr D. Williams of the Hitachi Cambridge Laboratory for a partial financial support to the present work.

### References

- [1] M. Y. Han *et al*, *Phys. Rev. Lett*, vol. **98**, 1–4 (2007).
- [2] C. Stampfer *et al*, *Appl. Phys Lett*, **92**, 012102 (2008).
- [3] D. C. Bell *et al*, *Nanotechnology*, **20**, 455301 (2009).
- [4] H. I. Beam *et al*, *ACS nano*, **3**, 2674–6, (2009).
- [5] A. C. Ferrari *et al*, *Phys. Rev. Lett* **97**, 187401 (2006)
- [6] S. Boden *et al*, Graphene 2011, Bilbao, Spain (2011)

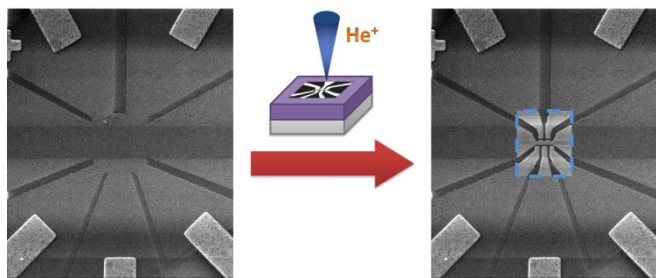


Fig.1 a) Conceptual demonstration of HIM based fabrication process of a double quantum dot (DQD) structure. The critical pattern in the center is carved onto pre-defined EBL structure using focused  $\text{He}^+$  beam.

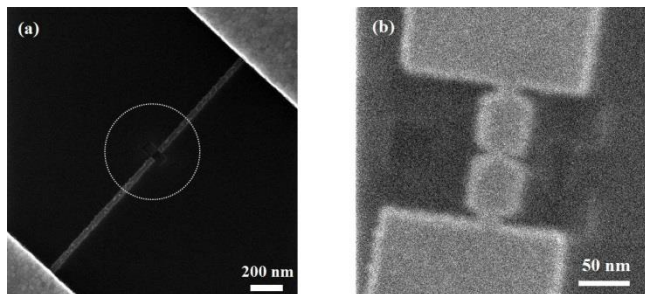


Fig. 2 Fabrication result on a double quantum dot (DQD) structure carved on a GNR. a) A GNR of  $150\text{nm}$  was prepared by EBL lithography and RIE etching. The circled labels the area where subsequent HIM milling is performed. b) A well-defined  $50\text{nm}$  DQD structure with  $25\text{nm}$  wide constrictions were then carved by HIM directly on the GNR.

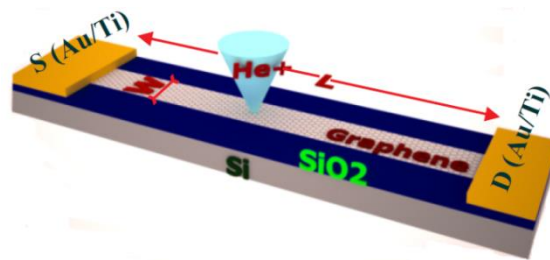


Fig. 3 The sketch of the device showing the BGFET channel, the radiating focused helium ion beam, the source, the drain and the dimensions of the channel. The highly doped silicon substrate is used as a control gate.

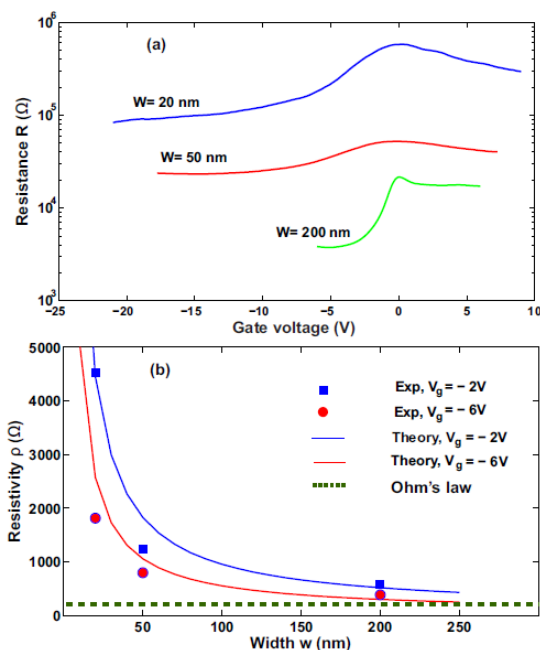


Fig. 4 a) Resistance of three BGFETs with widths of  $20\text{ nm}$ ,  $50\text{ nm}$  and  $200\text{ nm}$  and a length of  $2\text{ m}$  as a function of the gate voltage, for  $V_d = 7\text{ mV}$ . The gate voltage is defined relative to the voltage at the neutrality point. b) Resistivity as a function of the channel width for two values of the gate voltage  $V_g = -2\text{ V}$  and  $V_g = -6\text{ V}$ . The solid lines show theoretical resistivity.

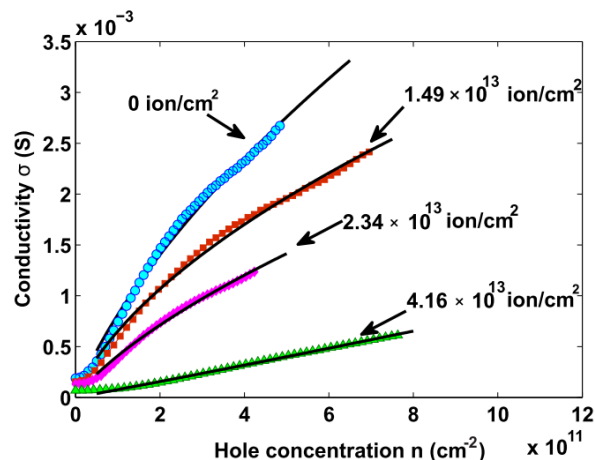


Fig. 5 Plots of the conductivity vs hole concentration for different doses as indicated. The continuous lines show calculated conductivity.